Volume 14, Issue 1, 142302 (1-9)

International Journal Industrial Chemistry (IJIC)

https://dx.doi.org/10.57647/j.ijic.2023.1401.02

Study of polyvinyl chloride/low density polyethylene wastes based blend

Mohamed Bouakkaz, Salim Djekhaba, Chaouki Bendjaouahdou*

Department of Industrial Chemistry, Biskra University, Algeria.

***Corresponding author**:chawk052000@yahoo.fr

Original Research

Received:
17 October 2022
Revised:
28 December 2022
Accepted:
2 February 2022
Published online:
30 March 2023

Abstract:

This research was aimed to study various PVC/LDPE blends in order to valorize the PVC and LDPE wastes by blending them. Indeed, this homopolymers constitute an important part of the plastic industry production in the world. The polymer blends were prepared by melt blending followed by extrusion. The obtained results showed that the mechanical properties were weak and an improvement of these properties occurs when the morphology evolves from matrix/droplets towards co-continued structure. The morphology is greatly related to the viscosity/volume ratio of each blend component. The increase of PVC onset first step degradation temperature Td1 as function of of the increase of LDPE concentration is assigned to macromolecular cross recombination reactions between PVC and LDPE radicals that occur during the heating. This study had allowed getting a composition blend of interesting mechanical and thermal properties despite the no use of a compatibilizer.

Keywords: Blend; Polyvinyl chloride; Polyethylene; Mechanical properties

1. Introduction

Physical blending of binary [1–3] or ternary [4] polymer systems is a practical route aiming to obtain a resulting blend which is expected to have the positive properties of each component. According to the continuity or discontinuity of constituting phases, A predictive scheme was proposed for the simultaneous calculation of the modulus and yield (or tensile) strength of ternary polymer systems [5, 6] The main objective to physical mix polyvinyl chloride (PVC) and low density polyethylene (LDPE) is to obtain a blend with the combined advantage of polyvinyl chloride and polyethylene. Indeed, the PVC resin is characterised by a satisfying break resistance and weak thermal resistance and the LDPE is characterised by a satisfying thermal and impact resistance and a weak break resistance. Since the PVC and the LDPE are extensively used in various domains, so the valorisation of their wastes by recycling them as a blend can constitute a concern for preserving the environment. So, the novelty of this work is to get some insights related to the morphology and properties of PVC/LDPE system and to study the properties of PVC/LDPE blend in order to try to valorise their wastes as a blend which it is expect to combine the synergistic effects of their positive properties. The choice of this system is due to the non similar properties of each individual polymer; their blend can lead to a new material having interesting properties. On the other hand, the route used for blending the components correspond to a common techniques used in the plastic industry (calendering followed by extrusion).

In the following paragraph, a short abstract will be presented about the main results obtained in the scientific literature related to PVC/LDPE blend. Ghafar and Scott [7] showed that for PVC/LDPE blends containing up to 20 wt % of PVC, the Young modulus increases as a function of PVC concentration meanwhile the tensile strength and the strain at break showed a minimum at 5 wt % of PVC and this behavior was explained by the variation of the blend morphology. It was also reported [6] that the morphology of PVC/LDPE blend having 50/50 wt % composition is related directly with the melt viscosity ratio of the components, and the control of this ratio is obtained by the variation of the mixer rotation speed. It was remarked [8] that the polymer which has the lower viscosity constitutes the continued phase and the morphology bi-continued is observed when the viscosities of the two components are closer. The blend having a bi-continued

morphology exhibits the highest values of break resistance and strain at break whereas, the blend having LDPE matrix (continued phase) exhibits the best impact resistance [8–10]. It was reported [11] that the compatibilization of PVC/LDPE blend by poly(hydrogenated butadiene-methyl methacrylate) copolymer is related to the combination of the copolymer molecular weight, copolymer concentration and the composition of the blend. The plasma processing [12] was applied to one of the components (LDPE) of PVC/LDPE blend in order to influence the degree of compatibility. Other research [13] investigates the structural changes of polyvinyl chloride (PVC) in melt-blends of a low-density polyethylene (LDPE) and polyvinyl chloride (PVC), and the effects of LDPE content and number of extrusion passes. It was found that the glass transition and decomposition temperature decreased with increasing number of extrusion. Influences of contents and molecular weights of low-density polyethylene (LDPE) on dioctylphthalate (DOP) plasticization in the poly(vinyl chloride) (PVC) plastisol were investigated using DMA and DSC [14]. Methods of improving the mechanical properties of poly(vinyl chloride)/linear low density polyethylene have been investigated as routes of reprocessing polymer wastes and it was found that chlorinated polyethylene was efficient additive for improving their tensile strength and processing behavior [15]. A research [16] was aimed to understand how LDPE content impacts the structure of PVC in PVC/LDPE foam blends and how it affects the glass-transition temperature (T_g) which provide information related to the structure of the blend. The co-cross-linking of polyvinyl chloride (PVC) and low density polyethylene (LDPE) was studied [17] by THF extraction, FTIR, and Dynamic rheological analysis. It was found that dicumyl peroxide (DCP) could neither induce the cross-linking of PVC itself nor cause PVC chains to cocross-link with LDPE. Another study [18] reports the effects of LDPE content, compatibilizer type and rubber-wood sawdust loading on the properties of the PVC/LDPE blend. The results suggested that as the LDPE content was increased the mechanical properties of PVC-LDPE blend gradually decreased due to poor interfacial adhesion. Several compatibilizer can be added to PVC/LDPE blend [19]. The results showed that the optimum mechanical properties of the blend could be obtained using Silane A-137, MAPE (maleated polyethylene) of 1% wt and 2% wt of wood sawdust. On the other hand, the degradation mechanism and mechanical properties of PVC in PVC-PE melt blends were studied and the effects of molecular architecture, content, and MFI of PE were evidenced [20]. The LDPE can be added to the recycled PVC in order to improve the properties of the resulted blend and consequently to valorize the PVC waste [21]. Organoclay can be added to PVC/LDPE blend as a compatibiliser in order to improve the interfacial interactions between PVC and LDPE components [22]. Chlorinated polyethylene and a copolymer of polyvinylchloride with polyethylene were used as compatibiliser in a blend of polyvinylchloride and polyethylene [23]. Synergistic effects of metal stearate, calcium carbonate, and recycled polyethylene were studied on thermo-mechanical behavior of polyvinylchloride [24]. Furthermore, the effects of palm leaf fiber [25] and wood flour [26] on polyvinylchloride and low density polyethylene were also studied. On the other hand, the thermophysical effects of date palm fibers and acrylonitrile butadiene rubber on polyvinylchloride/low density polyethylene blend were recently reported [27]. Finally, it is worth to notice that polyvinylchloride/high density polyethylene blends are equally extensively studied [28–30].

2. Material and methods

2.1 Material

Wastes of PVC compound was used as the blend major constituent. The PVC had a density equal to 1.4 kg/m^3. Wastes of a low density polyethylene were used as a second component of the blend. The polyethylene had a density equal to 0.9 kg/m^3 and a melt flow index (MFI) equal to 1.2 g/10 min.

2.2 Preparation of the sample

The PVC and LDPE wastes were melt- blended, at 130°C in a two-roll mill (BRABENDER POLYMIX 200P, Germany). The twin-roll mill had a nip clearance of 0.5 mm and a friction ratio of 1.3 (20/15 rpm).

The blending started by mixing polyethylene (LDPE) on the two- roll mill for 10 min; then, the polyvinyl chloride wastes were added during 5 min. Finally, the resulted blend was extruded in a single- screw extruder. The used monovis extruder was a SCHWABENTHAN PLE 330 (Schwabenthan, Germany); it had a length/diameter ratio of 21, a diameter of 20 mm, a thread thickness of 5.4 mm, and a step between two successive threads of 15 mm. The barrel temperatures (from feed zone to die) and screw speed were set, respec-

Table 1. Weight composition of the PVC/LDPE formulations.

Sample code (PVC/LDPE)	PVC (g)	LDPE (g)
0/100	0	300
20/80	60	240
30/70	90	210
40/60	120	180
50/50	150	150
60/40	180	120
70/30	210	90
80/20	240	60

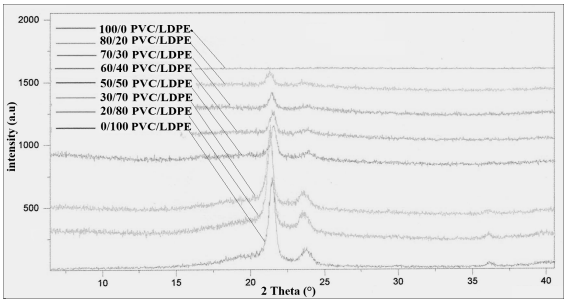

Figure 1. XRD patterns of PVC/LDPE blends.

tively, at 145–150–150°C and 35 rpm. Eight formulations were studied. In each formulation the total weight of the blend was constant and equal to 300 g (Table 1).

2.3 Characterizations

Tensile tests were done at ambient temperature (25 ± 2°C) according to ASTM D-638 standard with a TIME WDW-100E (TIME Ltd, China) testing machine. The dumb-bell shaped specimens (kind 5A, ISO 527-2) were extended at 50 mm/min cross head speed. The reported values of the tensile strength and strain at break were averages of five tests. The standard deviations were 2 % for the tensile strength and Young 's Moduli, and 5 % for the strain at break. The dumb-bell shaped samples were cut from 2 mm thick sheets that were obtained by compression moulding.

X-ray diffraction measurements (WAXD) were conducted on an BRUKER D8 ADVANCE (BRUKER, England) diffractometer operating at 40 KV and 40 mA in a continuous mode. The Incident ray had a wavelength of 1.54 $\AA$ generated by a CuK$_\alpha$ anode. The blend specimens analyzed by X-ray diffraction were films of 0.5 mm thickness obtained by compression molding at 140 °C.

The thermal stability of the PVC/LDPE blends was investigated by thermogravimetric analysis (TGA) and differential thermogravimetric analysis (DTGA) performed with a TA SDT Q600 (TA instruments, England) under a N_2 atmosphere (20 mL/ min) at the rate of 10°C/min with a sample weight equal to 10 mg.

Optical microscopy observations (OM) were done with a SHANDONG BIOBASE (SHANDONG, China) optical microscope in transmission light mode. The observed interface samples were PVC/LDPE fractured surface obtained at the end of the tensile tests.

DSC measurements were carried out under nitrogen on a TA DSC 2920 (TA instruments, England) apparatus. For each formulation, samples of 10 mg weight were analyzed. Each specimen was held at room temperature (23 °C) for 5 min before heating to 180 °C at a heating rate of 10 °C/min.

The FTIR (Fourier Transform Infra Red) analysis was done with a SHIMADZU FTIR -8400S (SHIMADZU Europe) spectrophotometer. The number of scans was equal to 64 in order to study the potential chemical changes or specific interactions inside the prepared samples.

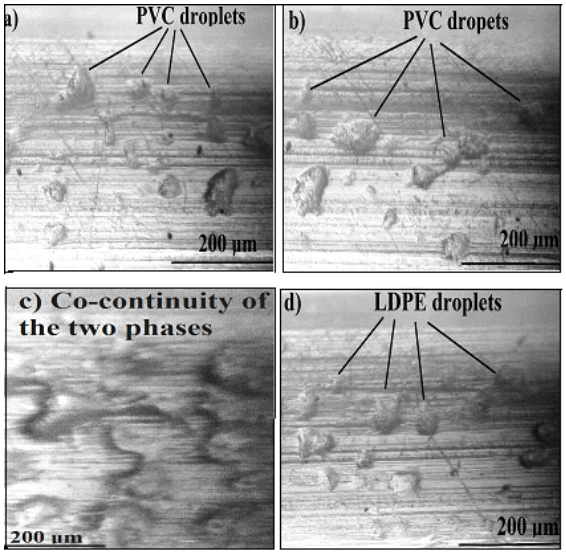

Figure 2. Optical microscopy micrographs of (a) PVC/LDPE (20/80), (b) PVC/LDPE (40/60), (c) PVC/LDPE (70/30), (d) PVC/LDPE (80/20).

3. Results and discussion

3.1 XRD analysis

From Fig. 1 it can be noticed that for neat polyethylene (lowest curve) there are three characteristic peaks of decreased intensity that correspond respectively to reticular diffraction peaks (110)(2θ = 21.42°), (200)(2θ = 23.76°), (020)(2θ = 36.08°). The intensity of these three peaks decreases proportionally with the diminution of the LDPE concentration in the blend and disappears completely for neat PVC (highest curve) which evidenced a fully lack of crystal domains for the PVC used in this study. The slight disturbance observed particularly for the first LDPE characteristic peak (110) for the studied blends relatively to neat LDPE occurs stochastically or randomly and it seems to be not significant (±0.15°) and not carrying any relevant information. Hence, in this study, the blending of amorphous PVC to crystalline LDPE does not affect the crystallinity of this last one. A similar result was also found for polypropylene/natural rubber immiscible blend [2].

3.2 Morphological characterization (optical microscopy observations)

Optical microscopy micrographs (Fig 2) show that there is a full immiscibility between PVC and LDPE components whatever the proportion of their respective phases and the morphology evolves with the blend composition. The LDPE rich blends (Fig 2a) exhibit a matrix/dispersed phase or nodular morphology characterized by a clear separation between the two phases; the LDPE constitute the continuous phase and the dispersed or droplet phase (nodules or inclusions) corresponds to the PVC particles having spherical or irregular form. These inclusions are bad dispersed in the LDPE matrix and are voluminous and can reach mean diameter of 100 μm for the rich LDPE blend (20/80). The matrix/droplets morphology observed for the PVC/LDPE blends (20/80) evolves gradually towards a co-

Table 2. Viscosity ratio $K(K = \alpha/\beta)$ of the PVC/LDPE formulations.

Sample code (PVC/LDPE)	PVC (%)	ϕ_{PVC} (%)	ϕ_{LDPE} (%)	α= η_{PVC}/ϕ_{PVC}	β= η_{LDPE}/ϕ_{LDPE}	Observed morphology
20/80	20	13.85	86.15	0.57	0.073	Continuous phase LDPE Dispersed phase PVC K=7.8
30/70	30	21.60	78.40	0.36	0.080	Continuous phase LDPE Dispersed phase PVC K=4.5
40/60	40	30.00	70.00	0.26	0.090	Continuous phase LDPE Dispersed phase PVC K=2.9
50/50	50	39.13	60.87	0.20	0.100	Continuous phase LDPE Dispersed phase PVC K=2.0
60/40	60	49.00	51.00	0.16	0.120	Continuous phase LDPE Dispersed phase PVC K=0.87
70/30	70	60.00	40.00	0.13	0.150	$\alpha \approx \beta$ co-continuity of the two phases K=0.87
80/20	80	72.00	28.00	0.11	0.220	$\alpha < \beta$ inversion of the two phases Continuous phase LDPE Dispersed phase PVC K=0.5

continuous one for more rich dispersed PVC phase blends (40/60, 70/30). This morphology evolution can be explained by the coalescence phenomenon of the PVC droplets up to the formation of entire domains of the same phase constituting a second continuous phase in the LDPE matrix. So, it can be observed for PVC/LDPE (40/60) blend (Fig 2b) a beginning of the continuity of the PVC phase with the existence of domains or nodules of relatively great dimension. For PVC/LDPE (70/30) blend (Fig 2c) it can be observed the lack of inclusions and a co-continuity of the two phases which are interpenetrated leading to a difficult distinction between the matrix and the dispersed phase. For PVC/LDPE (80/20) blend the PVC phase becomes so important that a phase inversion occurs and the PVC phase becomes the matrix and the LDPE domains becomes the dispersed phase (Fig 2d). Many researchers [31–36] have tried to predict theoretically the morphology of the immiscible polymeric blend as a function of the volume fraction (ϕ) and the viscosity (η) of the blend components. It was reported in the scientific literature [37–43] that the component which possesses the highest volume fraction and the lowest viscosity will constitutes the continuous phase. In case where one constituent has the highest volume fraction and the highest viscosity, the continuous phase will be related to the component having the smallest η/ϕ ratio. If the ratio η/ϕ of the continuous phase is equal to the viscosity ratio (η/ϕ) of the dispersed phase, the co-continuity of the two phases will be perfect (100% of co-continuity). By using the density values of the used PVC and LDPE (dPVC = 1.4 and dLDPE = 0.9) and considering the viscosity values η_{PVC}= 7.9 and η_{LDPE} = 6.3 determined in the same conditions relatively to the blends considered in this study by Fang et al.[8], the theoretical predictions based on the viscosity ratio applied to the studied blends leads to the results presented in Table 2.

From Table 2, it can be noticed that the theoretical predictions of the morphology are in good agreement with the optical microscopy observations. Particularly, it can be noticed that the theoretically predicted co-continuous morphology ($\alpha \approx \pm\beta$) for PVC/LDPE (70/30) blend is in good agreement with the observed one. On the other hand, when the observed morphology evolves gradually from nodular or droplet (50% of PVC) towards co-continuous one (70% of PVC), the $\alpha/\pm\beta$ ratio value is not very far from the unity ($0.87 \leq \alpha/\pm\beta \leq 2$).

3.3 FTIR analysis

Figure 3 shows the FTIR spectra of PVC/LDPE (30/70), PVC/LDPE (50/50) and PVC/LDPE (80/20) blends. It can be observed from Fig. 3 that all spectra of the blends are nearly superimpossible and they exhibited the characteristic bands of neat polymer. Furthermore, in Fig. 3, all the spectra show none moving, or disappearance of bands which is an indication of a total lack of chemical interactions between the two polymeric phases (PVC and LDPE) of the binary blend [31, 32].

3.4 DSC analysis

The percent or degree of crystallinity (χ_c) of the blends was estimated by the following equation [24]

$$\chi_c(\%) = \Delta H_f/(\Delta H_f^o.W_{PE}).100 \quad (1)$$

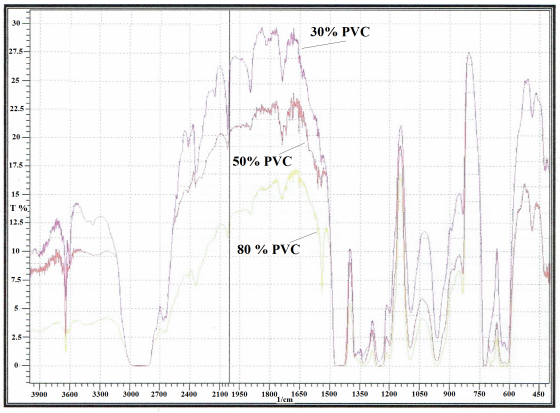

Figure 3. FTIR spectra of PVC/LDPE (30/70), PVC/LDPE (50/50) and PVC/LDPE (80/20) blends.

where ΔH_f is the enthalpy of the analyzed sample (J/g), WPE is the weight fraction of LDPE in the blend, ΔH_f^o is the enthalpy corresponding to the standard thermal crystallization of 100 % crystalline sample. For LDPE, the ΔH_f^o is equal to 293 J/g [42]. The results obtained by DSC analysis are summarized in Table 3. It can be noticed from Table 3 that for all LDPE based formulations the fusion temperatures are close to neat LDPE one (111.6 °C), the only noticeable difference is observed for 80 wt % LDPE based blend (107.0 °C) which is seemed due more to uncertainties related to the measuring of T_f since the crystallinity remains constant for all LDPE based blends. Furthermore, the glass transition temperature (T_g), which is a measure of the macromolecules mobility restriction [43], was not detected for less rich PVC blends and this effect is not due to the disappearance of this temperature but to the shift of this temperature (T_g) towards high values when the concentration of PVC decreases in the blend leading to the superposition of the glass transition phenomenon with the LDPE melting start leading to a difficult distinction between the two thermal effects. On the other hand, the influence of composition blend on T_g is important and we get the following sequence: $T_{gLDPE} < T_{gPVC} < T_{gPVC/LDPE(50/50)} < T_{gPVC/LDPE(80/20)}$. These results are in good agreement with the results obtained by Dickie [44–46], which he related the T_g variation to the morphology of immiscible binary blend of soft polymer/hard polymer kind, and it was found that the T_g value

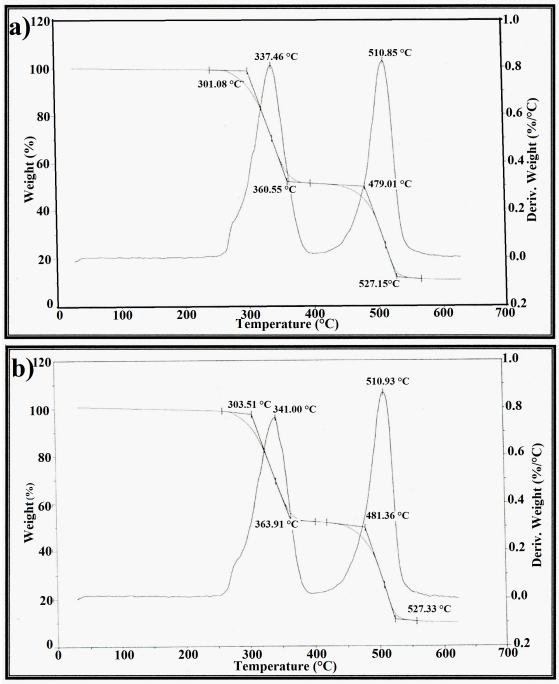

Figure 4. Thermograms (TGA/DTGA) of (a) PVC/LDPE (80/20) and (b) PVC/ LDPE (70/30) blends.

of the two phases is shifted towards high values when the soft phase constitutes the matrix (LDPE, and 50 % PVC based blend in this study); the T_g value of the two phases is shifted towards low values when the hard phase constitutes the matrix (PVC, and 80 % PVC based blend in this study). Furthermore, the decrease of T_g when the concentration of PVC increases from 50 to 90 wt. % is an indication of a slight miscibility of the two polymers [47]. It is worth to notice that in this study, only the T_g of the PVC phase was detected and the T_g of the LDPE was not detected in the experimental conditions.

3.5 Mechanical properties

Table 4 shows a dramatically fall of strain at break values as a function of PVC loading, .i.e. from 500 % for neat LDPE up to 6.48 % for PVC/ LDPE (40/60) composition, and then level off to approximately 3 % beyond 50 % of PVC loading. Young's moduli or tensile moduli, being a com-

Table 3. DSC parameters of the PVC/LDPE formulations.

Sample code (PVC/LDPE)	PVC %	ΔH_f J/kg	Crystallinity χ(%)	T_g °C	T_f °C
0/100	0	93.26	32.16	n.d*	111.6
20/80	20	73.94	31.87	n.d*	111.3
30/70	30	65.27	32.15	n.d*	111.3
40/60	40	54.46	31.30	n.d*	110.9
50/50	50	43.18	29.78	88.8	109.9
60/40	60	35.05	30.21	86.3	109.3
70/30	70	25.57	29.40	85.4	109.1
80/20	80	18.13	31.26	81.5	107.0
100/0	100	-	-	84.32	n.d*

*nd:not detected

Table 4. Mechanical properties of the PVC/LDPE formulations.

Sample code (PVC/LDPE)	PVC (%)	Young's moduli (MPa)	Tensile strength (MPa)	Strain at break (%)
0/100	0	149.0	9.5	500.0
20/80	20	100.0	6.2	75.0
30/70	30	130.0	6.3	40
40/60	40	350.0	6.4	7.0
50/50	50	520.0	6.9	2.5
60/40	60	530.0	11.8	3.0
70/30	70	550.0	12.0	3.0
80/20	80	560.0	12.2	3.0
100/0	100	676.0	37.6	6.7

bination of tensile strength and strain at break, measuring the stifness of the materials, it can be observed that the values of the tensile moduli of PVC/ LDPE (20/60) and PVC/ LDPE (30/70) blends are not different from neat LDPE one (weak stifness) and the tensile moduli value increases for more PVC containing formulations (increasing stifness). These observations are in good agreement with previous optical microscopy results indicating that PVC inclusions or nodules do not impact the LDPE in the blends which have LDPE matrix/PVC nodular inclusion (20 % and 30 % PVC). The sudden stifness improment of the blends is due to the adding of the stiff PVC and also to the occurrence of a co-continuous morphology, even partially. It can be remarked that 50/50, 60/40 and 70/30 blends exhibit the best balanced mechanical properties and can constitute a groundwork or foundation for future researches in order to improve the adhesion of the two polymeric phases by adding an appropriate compatibiliser.

3.6 Thermal stability

Generally, it was found in this study that the thermogrammes of all the blends show two degradation steps. For example, Fig 4 shows the TGA/DTGA thermogram of PVC/LDPE (80/20) and PVC/ LDPE (70/30) blends. These thermogrammes exhibit a first degradation step in the temperature range between 300 and 367 °C corresponding to the mass loss of PVC by the dehydrochlorination process [48], leading to the formation of polyenes which can reticulate and degrade at highest temperatures [49]. A second degradation step occurs in the temperature range between 480 and 530 °C corresponding to the degradation of polyene which appeared in the first degradation step. This polyene degradation seems to occur at the same temperature range of the polyethylene degradation as shown by Fig. 5.

It can be noticed in Fig 6 that the onset first step degradation temperature (T_{d1}) is function of the blend composition. This temperature (T_{d1}) exhibits à maximal value at 309.54 °C for PVC/ LDPE (80/20) blend and it decreases gradually with the increase of the PVC concentration in the blends with a singular point corresponding to a value of 298 °C. The increase of PVC T_{d1} as function of the increase of LDPE concentration is assigned to macromolecular cross recombination reactions between PVC and LDPE radicals that occur during the heating [49].

It was reported [40] by using 13C-NMR spectra analysis that these cross recombination reactions can lead to the formation of LDPE graffed by PVC (PVC-g-LDPE) structures. Figure 8 shows the variation of the duration of the first step degradation (t_1) as a function of the PVC loading in all studied blends. This duration (t_1) is calculated from the following equation

$$t_1 = [T_{f1} - T_{d1}] \times \frac{60}{\beta} \qquad (2)$$

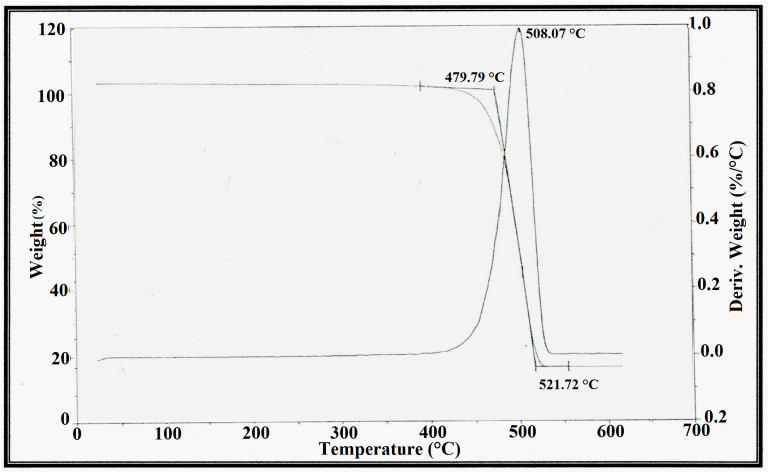

Figure 5. Thermograms (TGA/DTGA) of neat LDPE polymer.

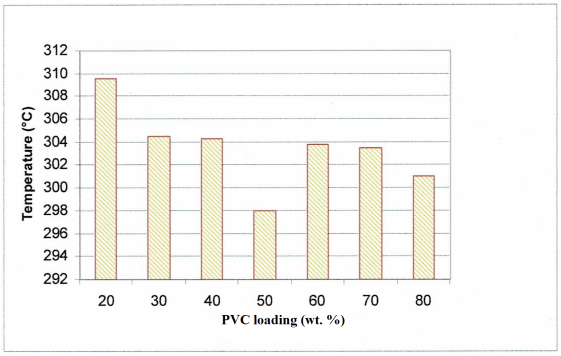

Figure 6. Onset first step degradation temperature (T_{d1}) as function of PVC loading.

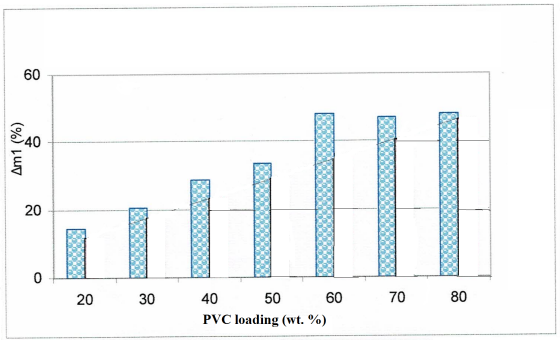

Figure 8. Weight loss during the first step degradation (Δ_{m1}) of PVC/LDPE blends as a function of the PVC loading.

In equation 2, T_{f1} is the final temperature of the first step degradation (expressed in °C), T_{d1} is expressed in °C, β is the heating speed (50°C/min). It can be noticed from Fig. 7 that t_1 increases with the PVC loading up to a maximum corresponding to PVC/ LDPE (50/50) blend and decreases beyond this composition.

Fig. 8 shows the weight loss during the first step degradation (Δ_{m1}) as a function of the PVC loading for the studied blends. It can be observed that the weight loss (Δ_{m1}) increases with the PVC loading up to a maximum corresponding to PVC/ LDPE (60/40) blend and then level off beyond this composition. This fact can be explained by the important thermal resistance confered by PVC to the blend when its concentration increases as this component possesses an important inherent thermal resistance [50].

Fig 9 shows the temperature at the maximal speed during the first step degradation (T_{d1m}) as a function of the PVC loading for the studied blends. It can be observed that this figure indicates a correlation between the morphology and the thermal stability of the blends. Indeed, it can be noticed that the temperatures at the maximal speed during the first step degradation correspond to the blends which exhibit a full (70 wt. % of PVC) or partially (50 and 60 wt. % of PVC) co-continuous morphology with a T_{d1m} values close to 340 °C and more lower values fort the blends having a matrix/droplets morphology with a mimimal value for 30 wt. % PVC concentration.

Concerning, the second thermal effect (second thermal degradation step), since this thermal degradation occurs in the same temperature range of the LDPE and the polyene chains formed during the first thermal degradation step, so, it is difficult to make any observations from TGA/DTGA curves. However, it can be noticed that all the blends have second step degradation temperatures (T_{d2}) more important than LDPE one, especially for 20, 30, 40, 50 and 60 wt. % PVC composition (Fig. 10). Furthermore, the final weight loss (Fig. 11) decreases as a function of PVC loading and level off to approximately 40% for compositions greater or equal to 60 wt. % and giving a final char residue equal to 10% (Fig. 4). This fact can be explained by the formation of a great quantity of non flammable three dimensional network which originate from polyenes as PVC loading increases [51].

4. Conclusion

In this work PVC/LDPE blends of different composition were prepared in order to study their morphologies and their thermal and mechanical behaviours. The optical microscopy analysis showed that PVC/LDPE blend is not miscible whatever was the composition of the polymeric phases with a gradual evolution, as a function of PVC loading, from a LDPE / droplets morphology for PVC/LDPE 20/80, 30/70 and 40/60 compositions towards a co-continuous one for PVC/LDPE 70/30 blend. A reversal phase phenomenon is observed for PVC/LDPE 80/20.

The FTIR analysis assessed the total immiscibility of the two constituents (PVC, LDPE) by the lack of chemical

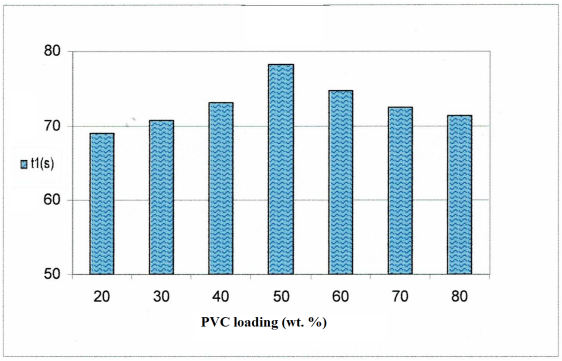

Figure 7. Duration of the first step degradation (t_1) as a function of the PVC loading.

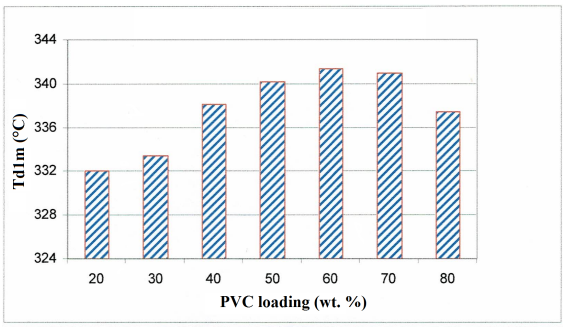

Figure 9. Temperature at the maximal speed during the first step degradation (T_{d1m}) as a function of the PVC loading.

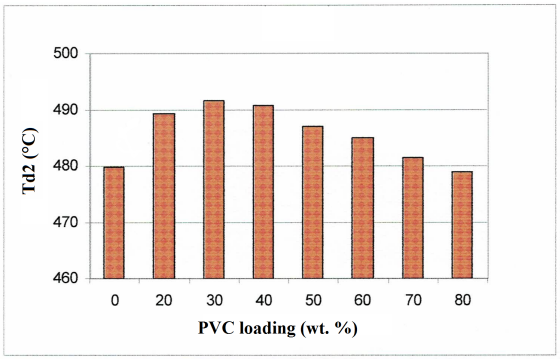

Figure 10. Onset second step degradation temperature (T_{d2}) as function of PVC loading.

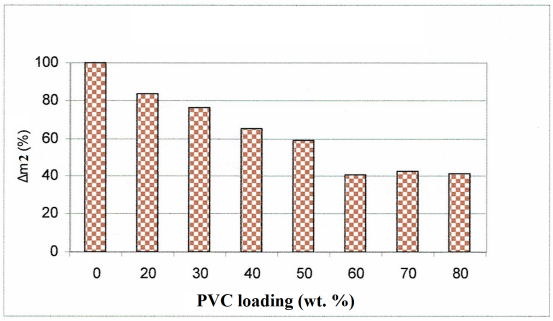

Figure 11. Weight loss during the second step degradation (Δ_{m2}) of PVC/LDPE blends as a function of the PVC loading.

interactions between the two polymeric phases. This lack of chemical interactions is confirmed by the DSC analysis which evidenced that the melting temperature and the neat LDPE cristalinity degree remains unchanged in all blend compositions (T_f = 109±2°C and X_c =30±2%).
The TGA/DTGA analysis showed a non monotone variation of thermal behaviour (T_{d1}, T_{d2} and Δ_m) as a function of blend composition. The high incompatibility character of the blends is traduced by weak mechanical properties (strength and Young's moduli), however, more improved when the morphology evolves from matrix/droplets to co-continuous one. The increase of PVC T_{d1} as function of of the increase of LDPE concentration is likely assigned to macromolecular cross recombination reactions between PVC and LDPE radicals that occurr during the heating and then leading to the formation of LDPE graffed by PVC (PVC-g-LDPE) which can play a role of compatibilizer. This study revealed a composition blend (70/30 PVC/LDPE) of well balanced mechanical and thermal properties which is an interesting method for recycling PVC and LDPE wastes.

Ethical approval:
This manuscript does not report on or involve the use of any animal or human data or tissue. So the ethical approval does not applicable.

Funding:
No funding was received to assist with conducting this study and the preparation of this manuscript.

Authors Contributions:
All authors have contributed equally to prepare the paper.

Availability of data and materials:
The data that support the findings of this study are available from the corresponding author upon reasonable request.

Conflict of Interests:
The authors declare that they have no known competing financial interests or personal relationships that could have appeared to influence the work reported in this paper.

Open Access

References

[1] C. Bendjaouahdou, S. Bensaad, and J. Vinyl. *Add*, **17**: 48, 2011.

[2] C. Bendjaouahdou and S. Bensaad. *Int J Ind Chem*, **9**: 345, 2018.

[3] C. Bendjaouahdou and S. Bensaad. *Energ Proceed*, **36**:574, 2013.

[4] F. Farahmand, P. Shokrollahi, and M. Mehrabzadeh. *Iran Polym J*, **12**:185, 2003.

[5] J. Kolarik, L. Fambri, A. Pegoretti, and A. Penati. *Polym Adv Tech*, **11**:75, 2000.

[6] J. Kolarik. *Polym Comp*, **18**:433, 1997.

[7] E. O. Khakberdiev, Q. N. U. Berdinazarov, D. A. U. Toshmamatov, and N. R. Ashurov. *J Vin Add Tech*, **28**: 659, 2022.

[8] Z. P. Fang, G. W. Ma, B. Q. Shentu, G. P. Cai, and C. W. Xu. *Europ Polym J*, **36**:2309, 2000.

[9] A. Ghaffar and G. Scott. *Europ Polym J*, **14**:631, 1978.

[10] K. Kroeze, G. Brinke, and G. Hadziioannou. *Polymer*, **38**:379, 1997.

[11] Z. P. Fang and G. W. Ma. *Chin J Polym Sci*, **24**:147, 2006.

[12] Q. Y. Zhou, B. H. Zhang, M. D. Song, and H. Bing-Lin. *Europ Polym J*, **32**:1145, 1996.

[13] G. Akovali, T. T. Torun, E. Bayramli, and N. K. Erinç. *Polymer*, **39**:1363, 1998.

[14] N. Sombatsompop, K. Sungsanit, and C. Thongpin. *Polym Eng Sci*, **44**:487, 2004.

[15] Y. T. Shieh and C M. Liu. *J Appl Polym Sci*, **83**:2548, 2002.

[16] J. Francis and K. E. George. *J Elastom Plast*, **24**:151, 1992.

[17] K. Roman and G. Zsoldos. *J Eng Manag Sci*, **4**:162, 2019.

[18] X. Luo, Z. Xu, and Z. Fang. *Polym Plast Tech Eng*, **45**:1271, 2006.

[19] J. Prachayawarakorn, J. Khamsri, K. Chaochanchaikul, and N. Sombatsompop. *J Appl Polym Sci*, **102**:598, 2006.

[20] J. Prachayawarakorn, S. Khunsumled, C. Thongpin, A. Kositchayong, and N. Sombatsompop. *J Appl Polym Sci*, **108**:3523, 2008.

[21] C. Thongpin, O. Santavitee, and N. Sombatsompop. *J Vinyl Addit Technol*, **12**:115, 2006.

[22] A. T. Sule, M. I. Aliko, K. S. Abdullahi, and M. S. Mato. *Afric Schol J Afric Sustain Dev*, **15**:147, 2019.

[23] M. Saeedi, I. Ghasemi, and M. Karrabi. *Iran Polym J*, **20**:423, 2011.

[24] E. O. Khakberdiev, Q. N. ugli Berdinazarov, D. A. ugli Toshmamatov, and N. R. Ashurov. *J Vinyl Addit Technol*, **28**:659, 2022.

[25] S. Maou, Y. Meftah, and A. Meghezzi. *Polyolefins J*, **10**:1, 2023.

[26] S. Maou, A. Meghezzi, N. Nebbache, and Y. Meftah. *J Vinyl Addit Technol*, **25**:88, 2019.

[27] M. Slimani, A. Meghezzi, Y. Meftah, and S. Maou. *Polyolefin J*, **10**:227, 2023.

[28] S. Maou, Y. Meftah, M. Tayefi, A. Meghezzi, and Y. Grohens. *J Polym Res*, **29**:161, 2022.

[29] S. Maou, Y. Meftah, Y. Grohens, A. Kervoelen, and A. Magurese. *J App Poly Sci*, **140**:e53781, 2023.

[30] S. Maou, A. Meghezzi, Y. Grohens, Y. Meftah, A. Kervoelen, and A. Magurese. *Ind Crop Prod*, **171**:113974, 2021.

[31] M. Beygi, S. N. Khorasani, P. Kamalian, M. Najafi, and S. Khalil. *Fibers Polym*, **23**:1975, 2022.

[32] D. Kathyanani, B. Manesh, N. A. Chamaraja, B. S. Madhukar, and B. Channe Gowda. *Coll surf A*, **649**: 129503, 2022.

[33] B. Manesh, H. R. Lokesh, D. Kathyanani, A. Sionkowska, D. Channe Gowda, and K. Adamiak. *Polym*, **272**:125833, 2023.

[34] G. N. Avgeropoulos, F. C. Weissert, P. H. Biddison, and G. G. A. Bohm Rub. *Chem Tech*, **49**:93, 1976.

[35] S. Hammani, N Moulai-Mostefa, P. Samyn, M. Bechelany, A. Dufresne, and A. Barhoum. *Polym Blend Mat*, **3**:926, 2020.

[36] M. S. Han, W. J. Seo, H. S. Paik, J. C. Hyun, J. W. Lee, and W. N. Kim. *Polym J*, **35**:127, 2003.

[37] I. S. Miles and A. Zurek. *Polym Eng Sci*, **28**:796, 1988.

[38] G. M. Jordhamo, J. A. Manson, and L. H. Sperling. *Polym Eng Sci*, **26**:517, 1986.

[39] P. Potschke and D. R. Paul. *J Macromol Sci Part C-Polym Rev*, **1**:87, 2003.

[40] R. Li, W. Yu, and C. Zhou. *J Macromol Sci Part B phys*, **45**:889, 2006.

[41] L A Utracki. *J Rheol*, **35**:1615, 1991.

[42] N. Sombatsompop, K. Sungsanit, and C. Thongpin. *Polym Eng Sci*, **44**:2004, 487.

[43] J .Cailloux, T. Abt, V. García-Masabet, O. Santan Perez, M. Sanchez-Soto, F. Carrasco, and M. L. Maspoch. *eXPR Polym Lett*, **12**:569, 2018.

[44] R. A. Dickie. *J App Polym Sci*, **17**:45, 1973.

[45] R. A. Dickie. *J App Polym Sci*, **17**:65, 1973.

[46] R. A. Dickie. *J App Polym Sci*, **17**:79, 1973.

[47] M. Kollar and G. Szoldos. *J Therm Ana Cal*, **107**:645, 2011.

[48] C. Bendjaouahdou and K. Aidaoui. *Polym Polym Comp*, **29**:949, 2021.

[49] V. N. Stipanelov, I. Klaric, and U. Roje. *Polym Degrad Stab*, **74**:203, 2001.

[50] W. H. Jr Starnes. *Prog Polym Sci*, **27**:2133, 2002.

[51] C. Thongpin, O. Santavitee, and N. Sombatsompop. *J Vin Add Tech*, **12**:115, 2006.